# Exact rainbow tensor networks for the colorful Motzkin and Fredkin spin chains

Rafael N. Alexander,[1,2] Amr Ahmadain,[2] Zhao Zhang,[2] and Israel Klich[2]
[1]*Center for Quantum Information and Control, University of New Mexico, Albuquerque, New Mexico 87131-0001, USA*
[2]*Department of Physics, University of Virginia, Charlottesville, Virginia 22903, USA*

(Received 11 January 2019; revised manuscript received 17 October 2019; published 24 December 2019)

We present bulk tensor networks that exactly represent the ground states of a continuous family of one-dimensional frustration-free Hamiltonians. These states, which are known as area-deformed Motzkin and Fredkin states, exhibit a novel quantum phase transition. By tuning a single parameter, they go from a phase obeying an area law to a highly entangled "rainbow" phase, where the half-chain entropy scales with the volume. Using the representation of these ground states as superpositions of random walks, we introduce tensor networks for these ground states where local and global rules of the walker are baked into bulk tensors, thereby providing an efficient description of the ground states (some of which satisfy a volume law scaling of entanglement entropy).

DOI: 10.1103/PhysRevB.100.214430

## I. INTRODUCTION

Tensor networks can offer efficient descriptions of quantum states of interest. They have been used to numerically study the behavior of correlations, entropy, and many other properties of quantum phases of matter (for a review see, e.g., [1]). Beyond their utility for numerical studies, they offer a convenient framework for classifying the complex structure of correlations of wave functions [2] and foster connections with coarse-graining methods, such as renormalization, and related topics in field theory, such as gauge-gravity duality [3]. Matrix product states (MPS) are a particularly simple class of one-dimensional (1D) networks used in the density matrix renormalization group (DMRG) procedure [4], successfully used in the numerical investigation of quantum phases in one dimension.

Another class of network states, specially tailored to describe scale-invariant systems, are represented by the multiscale entanglement renormalization ansatz (MERA) [5,6]. MERA is used to represent approximate ground states of 1D quantum spin chains at criticality described by two-dimensional (2D) conformal field theory (CFT) [7]. The scale invariance of the MERA network turned out to also play a special role in connecting it to holographic duals in the sense of the AdS/CFT correspondence [3]. Here, the bulk of a MERA network can be understood as a discrete realization of three-dimensional (3D) anti–de Sitter space ($AdS_3$), identifying the extra holographic direction with the renormalization group (RG) flow in the MERA [3].

We stress that the above treatments look for *approximate* solutions of the actual ground states. Moreover, away from 1D gapped or conformal critical points, where the MPS and MERA have been extensively studied, relatively little is known. In particular, the interpretation and use of gauge-gravity dualities beyond CFTs is not very well understood and still under intense investigation. Thus, it is of great interest to find insightful examples for networks that describe exactly ground states of Hamiltonians beyond MPS and MERA.

In this article, we present a first example of an *exact* continuous family of networks that describe ground states of short-range local Hamiltonians across a phase transition from area law to volume entanglement scaling. These allow us to observe regimes associated with entanglement entropy ranging from bounded and logarithmic all the way to extensive. Our result is a complimentary construction to a recent example [8] of a scale-invariant network for the colorless version of the models described here, with a critical point featuring a transition between area law states through a critical point with a logarithmic entropy scaling.

We note that an explicit construction of a type of exact holography was recently achieved by mapping the Hamiltonian of free fermions on a circle onto a "bulk" free fermion Hamiltonian inside the disk with a hyperbolic metric [9], however, here we are interested in exact tensor network descriptions. We note that a related series of *approximate* constructions of a MERA for free fermions was shown in Refs. [10,11].

Our tensor network describes the ground states of the colorful and area-deformed Motzkin and Fredkin models. Motzkin models have been introduced as a new class of exactly solvable ground states of frustration-free quantum spin chain Hamiltonians [12,13]. A model with a similar behavior based on Fredkin gates has been introduced in Refs. [14,15]. The Motzkin model represents an example of systems not described by a CFT and thus, present a playground where new ideas that go beyond the MERA can be explored. Moreover, they admit a class of solvable deformations, the area deformed Motzkin model, discovered in Ref. [16], with a new phase transition and simple geometric interpretation. Further studies of Motzkin and Fredkin models have explored their possible relation to non-CFT field theories [17], the framework of symmetric inverse semigroups [18], and approximate quantum error-correcting codes [19].

Figure 1 describes schematically the remarkable quantum phase diagram of this model: As a function of the parameter $t$, the area-deformed Motzkin model may be tuned all the way

 

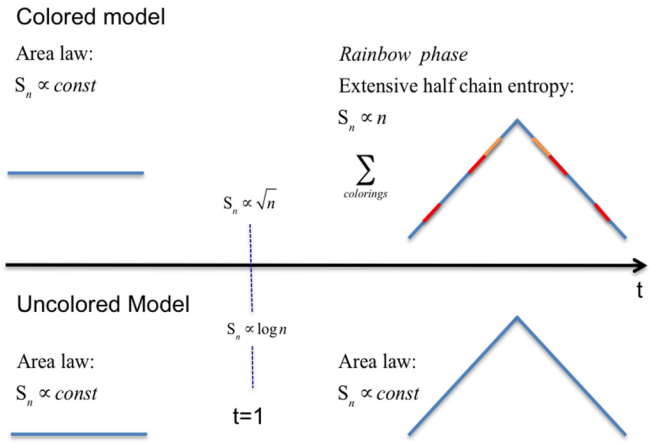


FIG. 1. Phase diagram for the area deformed Motzkin model.

between a gapless critical phase with volume law entropy scaling, to a gapped phase obeying an area law, passing through critical points obeying logarithmic or square root entanglement scaling depending on the size of the local Hilbert space. The model at hand has a geometrically appealing description that relates 1D wave function amplitudes to objects in a 2D space.

Of particular interest is the high "half-chain" entropy phase, the "rainbow" phase, where the state approximates a superposition of concentric entangled pairs about the middle of the system. The highly nonlocal nature of the rainbow phase precludes its local efficient description in terms of either MPS or MERA, and necessitated developing the new network that we present here. Apart from the deformed Motzkin and Fredkin models, which are translationally invariant in the bulk, a rainbow type ground state may also appear in spatially inhomogeneous models. Indeed, such a phase was first demonstrated by Vitagliano *et al.* in [20] for a spin chain with an explicitly broken bulk transitional invariance via exponentially varying coupling constants. The concentric singlet phase was shown in the strong coupling limit [20], where the model was analyzed using a Dasgupta-Ma real-space renormalization group technique, and also studied in [21–23] and via mapping to free fermions and exact diagonalization.

## II. THE MOTZKIN MODEL

The Motzkin model is a one-dimensional spin-$j$ chain ($j$ integer). For $j = 1$, identifying each local spin basis state $\{|1\rangle, |0\rangle, |-1\rangle\}$ with a line segment $\{\diagup, —, \diagdown\}$, respectively, allows us to represent states as a superposition of walks. Higher dimensional spins can be analogously defined using colored walks. For example, for $j = 3$, the basis states $\{|3\rangle, |2\rangle, |1\rangle, |0\rangle, |-1\rangle, |-2\rangle, |-3\rangle\}$ are identified with $\{\diagup, \diagup, \diagup, —, \diagdown, \diagdown, \diagdown\}$, respectively.

The Motzkin model has a unique, zero-energy frustration free ground state. For the spin $j > 1$ ($j = 1$) case, this ground state is a superposition of walks called "colored (uncolored) Motzkin walks." A Motzkin walk $w$ is a walk on the $\mathbb{Z}^2$ lattice using the line segments $\{\diagup, —, \diagdown\}$ that starts at (0,0), goes to $(2n, 0)$, and never goes below the $y = 0$ line. In the colored walks, all upwards steps have an arbitrary color. However, the color of a downward step $(k, m) \to (k + 1, m - 1) \in w$ must match the color of the most recent upwards step occurring at the same height; i.e., $\text{color}((k, m) \to (k + 1, m - 1)) = \text{color}((l, m - 1) \to (l + 1, m))$ where $l = \max(l')$ s.t. $l' < k$ and $(l', m - 1) \to (l' + 1, m) \in w$. Denoting the set of colored Motzkin walks with $c$ colors on $2n$ steps $\mathcal{M}_c^{2n}$, the ground state can be written as

$$|\Psi(t)\rangle = \frac{1}{\mathcal{N}} \sum_{w \in \mathcal{M}_c^{2n}} t^{\mathcal{A}(w)} |w\rangle. \tag{1}$$

Here $\mathcal{A}(w)$ denotes the area below the Motzkin walk $w$, and $\mathcal{N}$ is a normalization factor. A similar type of ground state occurs in the Fredkin models, which are half-integer spin models that have essentially the same structure, but without the "flat" move [14,24–26]. The half-chain entropy is easily understood from observing the dominant Motzkin walks in the limits of $t \to \infty$ and $t \to 0$ and is described in Fig. 1. The deformed Motzkin and Fredkin walks can naturally be viewed as constrained trajectories of a random walker in the presence of drift, with the "$x$" axis playing the role of time.

The area deformed colorful Motzkin state is the ground state of a local frustration-free Hamiltonian. It is defined on a spin chain with $2n$ sites as follows:

$$H = \Pi_{\text{boundary}} + \sum_{j=1}^{2n-1} \Pi_j + \sum_{j=1}^{2n-1} \Pi_j^{\text{cross}}, \tag{2}$$

where $\Pi_j$, $\Pi_j^{\text{cross}}$ act on the pair of spins $j$, $j + 1$ with

$$\Pi_j = \sum_{k=1}^{s} \left( \left|\Phi_t^k\right\rangle\left\langle\Phi_t^k\right|_{j,j+1} + \left|\Psi_t^k\right\rangle\left\langle\Psi_t^k\right|_{j,j+1} + \left|\Theta_t^k\right\rangle\left\langle\Theta_t^k\right|_{j,j+1} \right), \tag{3}$$

$$\Pi_j^{\text{cross}} = \sum_{k \neq k'} |u^k d^{k'}\rangle\langle u^k d^{k'}|, \tag{4}$$

$$\Pi_{\text{boundary}} = \sum_{k=1}^{s} (|d^k\rangle\langle d^k|_1 + |u^k\rangle\langle u^k|_{2n}), \tag{5}$$

where $\Phi^k$, $\Psi^k$, $\Theta^k$ are the following states on pairs of neighboring spins,

$$\left|\Phi_t^k\right\rangle \propto |u^k 0\rangle - t|0u^k\rangle\,; \; \left|\Psi_t^k\right\rangle \propto |0d^k\rangle - t|d^k 0\rangle; \tag{6}$$

$$\left|\Theta_t^k\right\rangle \propto |u^k d^k\rangle - t|00\rangle. \tag{7}$$

## III. EXACT REPRESENTATION VIA THE RAINBOW TENSOR NETWORK

### A. Walks as tiles

Motivated by the correspondence by the state and walks, we introduce a network representation where the rules of the walk are built into the fundamental tensors. To do so, we first represent the possible walks as a collection of possible tilings showing colored arcs or "rainbows." Consider the set of tiles shown in Fig. 2(a). These can be used to tile a square lattice. We say that a tiling is *valid* if the edges of each tile match, and if the following boundary conditions are satisfied: all northern, eastern, and western boundary edges must take the value $\omega$,

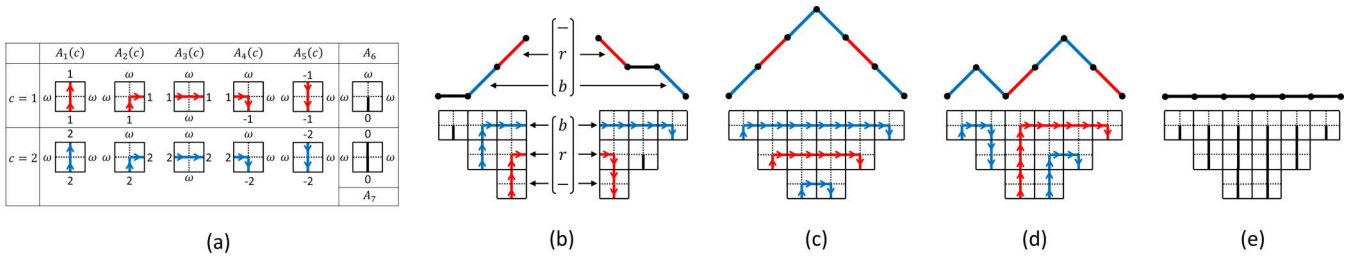


FIG. 2. (a) Twelve tiles for the spin-2 case. In the spin-$j$ case, there will be $j$ differently colored copies of each arrowed tile (there are five distinct arrowed configurations). (b)–(e) Examples of the mapping between colored walks (top) and full packing of paths in the bulk of the network (bottom). The sequence of paired line segments along a vertical cut in the walk (top) mirrors the pairing of walk segments across the same in the grid (bottom). This is shown explicitly in (a).

and all southern boundary edges are prohibited from taking the value $\omega$.

The set of length $2n$-colored Motzkin walks is isomorphic to the set of valid tilings of an inverted step pyramid. Examples are shown in Figs. 2(b)–2(e). Each valid tiling corresponds to a full packing of the interior of the square grid by nonintersecting arrowed and arrowless paths. The arrowed paths begin traveling straight upwards from the bottom of the grid, take two right turns (following a $\Pi$-shaped path), and return to the bottom of the grid. The arrowless lines form straight vertical paths from the bottom of the grid and terminate in the interior. Each colored walk is isomorphic to a configuration of colored nonintersecting chords that join $2n$ points that lie on a circle. See Fig. 3(a) for an example. Flattening the circle—as shown in Fig. 3(b)—results in a configuration of nested colored arcs. These are "smoothed" counterparts of configurations of $\Pi$-shaped paths that pack the square grid, as shown in Fig. 3(c). Each tiling is uniquely specified by the numerical values on the southernmost horizontal edge of each column (recall that the value $\omega$ is prohibited). For the tiling to be valid, each path seeks to maximize the height it reaches in the interior.

### B. Tiles as tensors

We introduce a network that is designed to sum over all valid tilings. Thus, it represents a sum over all Motzkin walks, and hence, the ground state of the Motzkin model.

The network is shown in Fig. 4. Physical indices are arranged along the bottom edge. The basic building block is the four-index tensor $B$, defined as

$$B(t) := \sum_{c=1}^{j} A_1(c) + \sqrt{t}A_2(c) + tA_3(c) + \sqrt{t}A_4(c) + A_5(c) + A_6 + A_7, \tag{8}$$

where the $A_i$ are four index tensors with north, east, south, and west facing indices denoted as $k_1$, $k_2$, $k_3$, and $k_4$, respectively. The entries of $A_i$ equal one when all $k_i$ values match the corresponding tile in Fig. 2(a), and are zero otherwise. Contracting a single index between two $B$ tensors corresponds to summing over tile configurations that match on the joining edge. To ensure that the boundary conditions of a valid tiling are met, we contract the indices on the north, east, and west boundaries of the network with the vector $|\omega\rangle$, and the legs on the south boundary with the projector $\Pi = I - |\omega\rangle\langle\omega|$.

Similarly, the ground state of the Fredkin model can be represented by walks that do not include any horizontal segments. The network shown in Fig. 4 can be re-purposed for such models if all tiles containing solid lines without arrows are removed from $B$. The new tensor is defined as

$$B'(t) := \sum_{r=\frac{1}{2}}^{j} \sum_{l=1}^{5} A_l(r,t). \tag{9}$$

In addition, we map nonzero integer spin values $j$ to half-integer values $j - \frac{\mathrm{sign}(j)}{2}$. The correspondence between walks and arrowed paths in the network is otherwise identical to the Motzkin case [see, e.g., Figs. 2(c) and 2(d)].

The rainbow network is an exact representation for any member of the family of colored and area-weighted Motzkin. The network provides an efficient description of any such state [only $O(n^2)$ many identical tensors are required to specify it]. Note that if each column of square tensors is viewed as

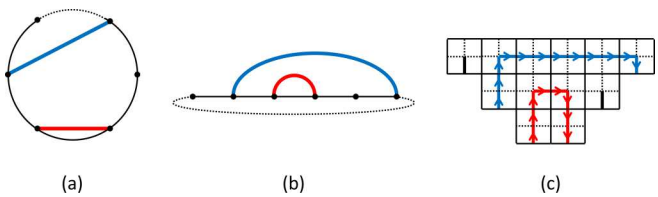


FIG. 3. Length $2n$ Motzkin walks are one-to-one with nonintersecting chords between $2n$ points on a circle. These, in turn, are one-to-one with full packings of the interior of an inverted step pyramid by paths of arrowed and arrowless lines.

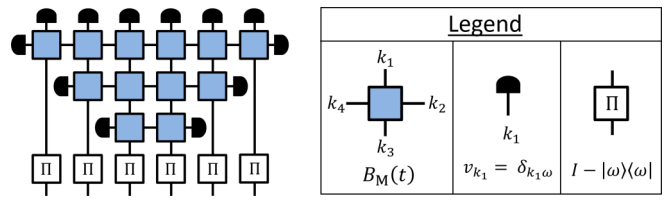


FIG. 4. Rainbow tensor network.

a single matrix, it yields an MPS with bond dimension that grows exponentially with the system size. Thus, this network does not readily provide an efficient means for computing expectation values of local observables.

### C. Encoding of correlations in the tensor network and dependence on t.

The horizontal virtual bonds across a cut between two columns of $B$ tensors store an ordered list of colors corresponding to unpaired walk segments across that cut in the walk. To see this, consider cutting a given walk between sites $z$ and $z+1$ at a height $h_z$. Then, exactly $h_z$ pairs of locations split by this cut are perfectly correlated in the color degree of freedom. Denote these pairs of sites by $(x_1, y_1)\ldots(x_{h_z}, y_{h_z})$, where $x_j \leqslant z < y_j$, $\forall j$. Assume these are ordered so that $x_1 < x_2 < \ldots x_{h_z}$ (and therefore, $y_{h_z} < y_{h_z-1} < \ldots y_1$), and denote the colors of these pairs by $c_1, c_2, \ldots c_{h_z}$. Correlations across the cut are encoded within these color configurations. This type of data structure is known as a *stack*; the upwards steps to the left of the cut are "undone" by a downwards step to the right of the cut in reverse order. In the network, the colors are stored in order $(c_1, c_2, \ldots)$ from top to bottom moving downwards along the cut. See Fig. 2(b) for an example.

The $B$ tensor in Eq. (8) explicitly includes the $t$ parameter. The tiles $\{A_l\}$ have a factor of $\sqrt{t}$ for every horizontal arrow segment that appears. As discussed above, the height/color information of each walk is stored in the horizontal virtual bonds between two columns of $B$ tensors. Therefore, for a given tiling, each horizontal arrow segment contributes half a unit of area. Scaling the tiles by the number of horizontal arrows, therefore, corresponds to scaling the walks by the number of area units they cover.

Beyond tensor networks for 1D quantum spin chains, such a geometric approach has been useful in many problems of statistical mechanics including quasicrystal spin glasses [27], dimer models, and spin jams [28] where the building blocks, the tiles, correspond to allowed local physical configurations and offer a convenient, graphical approach to tensor networks where a geometrical picture of the state is involved.

## IV. DISCUSSION

The construction of a homogeneous MERA tensor network is special in ways that do not always extend to systems without scale invariance or logarithmic scaling of entanglement entropy. In a MERA, tensor elements obtained numerically are *generic*, therefore, generic correlations between a pair of operators acting at positions $x_1$ and $x_2$ are carried through the bonds/links of the network [29], giving

$$G(x_1, x_2) \approx e^{-\alpha D(x_1, x_2)} \tag{10}$$

for some correlation function $G(x_1, x_2)$, where $D(x_1, x_2)$ is the graph distance (i.e., minimal number of edges) between $x_1$ and $x_2$ within the tensor network, and $\alpha$ is a positive constant that depends on the operators in question. Since in a MERA, $D(x_1, x_2) \approx \log(|x_1 - x_2|)$, it follows from Eq. (10) that $D(x_1, x_2)$ dictates a power law scaling of $G(x_1, x_2)$ as expected for a CFT. From the point of view of the network structure, MERA may be naturally seen as a type of holographic description. In particular, it clearly demonstrates features such as consistency with the Ryu-Takayanagi (RT) formula [30], relating entanglement entropy of a region with its minimal bounding surface in the holographic direction. For nonconformal field theories, a holographic gravity dual may not, in general, be able to simultaneously satisfy an RT-like formula for entanglement entropy and a semiclassical description of correlation functions given in terms of geodesics. Note that, as mentioned before, the gap scaling behavior shows that even the colorless Motzkin system, where entropy behaves logarithmically, is not a CFT [12,31]. Indeed, a corresponding field theory has yet to be properly described. Interestingly, Chen *et al.* [17] found two gapless modes with different dynamical scaling exponents, $z = 2.7$ and $z = 3.16$, respectively, which they argue is evidence for multiple dynamics. They also constructed a continuum limit of the colorless Motzkin ground state as a ground state of a $z = 2$ Lifshitz scalar field theory with orbifold boundary (note that due to the mismatch in dynamical scaling, this $z = 2$ Lifshitz field theory is insufficient to fully describe the spectrum of the Motzkin spin chain).

What about the tensor network we presented here? Viewed as a graph, it is defined on a square grid, that seems to correspond to a "flat" holographic metric. However, if we compute correlation functions, they are strongly dependent on position. In particular, in the $t \to \infty$ limit, correlation functions represent concentric pairs of maximally entangled pairs. The corresponding holographic geometry is perhaps more appropriately represented as an array of concentric "wormholes" [32,33], i.e., a rainbow. Another possibility is to start from a CFT in an appropriate curved background metric when looking for a holographic dual. Such a metric comes out naturally in the fermionic rainbow chain, where the couplings are strongly spatially in-homogenous; see, e.g., [22].

For example, consider the correlations between color degrees of freedom. We concentrate on the $t \to \infty$ limit, where the Motzkin walk is characterized by a tall triangular mountain with small corrections. In this case the "up-down" degree of freedom of the spins is almost frozen, however, colors are widely fluctuating via completely correlated pairs symmetric about the middle of the chain. To quantify the correlations, we will assume two colors, say red and blue. Here the local Hilbert space is five dimensional, consisting of the local states

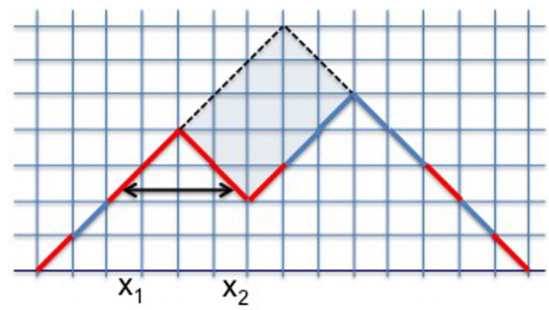


FIG. 5. This path contributes to the color correlation of spins $x_1$ and $x_2$ with maximal area.

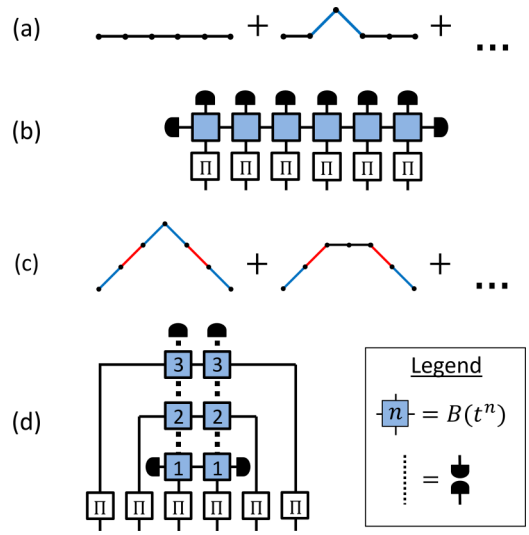


FIG. 6. (a) For fixed $n$, and $t \to 0$, the ground state can be approximated by discarding walks that have area $\geqslant 2$, i.e., keeping only the flat walk plus all colorings of area 1 walks. (b) Such walks are contained within the tensor network shown, which can be viewed as a truncated rainbow tensor network. The geometry of this network is the same as an MPS. (c) For fixed $n$, and $t \to \infty$, the ground state can be approximated by discarding walks that have area $\leqslant (n^2 - 2)$. (d) Such walks are contained within the tensor network shown, similar to an alternately truncated rainbow network.

$\downarrow, \uparrow, \downarrow, \uparrow, -$. We can define a color operator $C$, by its action:

$$C|s\rangle = \text{color}(s)|s\rangle, \tag{11}$$

where $\text{color}(\downarrow, \uparrow) = -1$, $\text{color}(\downarrow, \uparrow) = 1$, and $\text{color}(-) = 0$ for the horizontal step. In the ground state $|\Psi(t)\rangle$, consider the color-color correlation function:

$$G_{x_1,x_2} \equiv \langle C_{x_1} C_{x_2}\rangle - \langle C_{x_1}\rangle\langle C_{x_2}\rangle = \langle C_{x_1} C_{x_2}\rangle. \tag{12}$$

Note that since the state has no particular color preference $\langle\Psi(t)|C_x|\Psi(t)\rangle = 0$ for any point $x$ and any value of $t$. If a holographic metric allows for a semiclassical description of the state we should expect

$$G_{x_1,x_2} \sim e^{-hD(x_1,x_2)}, \tag{13}$$

where $D$ is the geodesic distance between $x_1$ and $x_2$ when going through the holographic geometry and $h$ is a parameter related to the scaling of our "color" operator.

In the $t \to \infty$ limit, the asymptotically leading contributions to the area weighted Motzkin walks are determined by maximal area walks that contribute to the correlation. Assuming $x_2 - x_1$ is even, a maximal area walk with mandatory $\text{color}(x_2) = \text{color}(x_1)$ is illustrated in Fig. 5. Choosing our coordinate system such that $x = 0$ corresponds to the middle of the spin chain, we get

$$G_{x_1,x_2} \sim \frac{2^n t^{2A_{\max}(w)}}{2^n t^{4n}} \sim e^{-h|x_1^2 - x_2^2|}, \tag{14}$$

with $h = \log t$. In the continuum limit we have

$$G_{x_1,x_2} \propto (\delta(x_1 - x_2) + \delta(x_1 + x_2)). \tag{15}$$

Thus, in a holographic metric describing this state, points that are symmetrical around the middle should be connected by short geodesics. On the other hand, in the limit $t \to 0$, the situation is reversed—there are only correlations between very close points. Appropriate approximate tensor networks are described in Fig. 6.

One interesting question in this regard is what the nature of a *bulk* Hamiltonian generating such superpositions is. It is quite clear that the rainbow network, for example, represents a bulk state that is unlikely to be generated by an exact local bulk Hamiltonian: It consists of a superposition of bulk rainbows that cannot be deformed to each other by local bulk moves. Is this a feature of the particular representation we found, or is it a general expectation that high entanglement ground states have to be associated with nonlocal bulk Hamiltonians?

## ACKNOWLEDGMENTS

We thank Glen Evenbly, Ramis Movassagh, Vladimir Korepin, and Xiao-Liang Qi for discussions. The work of I.K., A.A., and Z.Z. was supported in part by NSF Grant No. DMR-1508245. The work of R.N.A. was partially supported by National Science Foundation Grant No. PHY-1630114.

## APPENDIX

### Color correlation functions

The color correlations in the colorful Motzkin model can be described via

$$G_{x_1,x_2} = \frac{\sum_{w\in\mathcal{C}_+} t^{2A(w)} - \sum_{w\in\mathcal{C}_-} t^{2A(w)}}{\sum_w t^{2A(w)}}, \tag{A1}$$

where we defined the sets:

$$\mathcal{C}_\pm(x_1, x_2) := \{w \in \mathcal{M}_s^{2n} : \text{color}(x_1)\text{color}(x_2) = \pm 1\}.$$

Consider a particular Motzkin walk in $\mathcal{C}_+(x_1, x_2)$. If in this walk the color in $x_2$ is independent of that of $x_1$ (for example, if in $x_2$ the step is upwards) then there will be a corresponding Motzkin walk in $\mathcal{C}_-(x_1, x_2)$ with the same area, and no contribution to $G_{x_1,x_2}$. Thus, walks where the colors of $x_1, x_2$ are not correlated will not contribute to the sum. We therefore write $G$ as

$$G_{x_1,x_2} = \frac{\sum_{w:\,\text{s.t. color}(x_1)=\text{color}(x_2)} t^{2A(w)}}{\sum_w t^{2A(w)}}. \tag{A2}$$

[1] R. Orús, Ann. Phys. (NY) **349**, 117 (2014).
[2] J. C. Bridgeman and C. T. Chubb, J. Phys. A **50**, 223001 (2017).
[3] B. Swingle, Phys. Rev. D **86**, 065007 (2012).
[4] S. R. White, Phys. Rev. Lett. **69**, 2863 (1992).

[5] G. Vidal, Phys. Rev. Lett. **99**, 220405 (2007).
[6] G. Vidal, Phys. Rev. Lett. **101**, 110501 (2008).
[7] R. N. C. Pfeifer, G. Evenbly, and G. Vidal, Phys. Rev. A **79**, 040301(R) (2009).
[8] R. N. Alexander, G. Evenbly, and I. Klich, arXiv:1806.09626.
[9] X.-L. Qi, arXiv:1309.6282.
[10] G. Evenbly and S. R. White, Phys. Rev. Lett. **116**, 140403 (2016).
[11] J. Haegeman, B. Swingle, M. Walter, J. Cotler, G. Evenbly, and V. B. Scholz, Phys. Rev. X **8**, 011003 (2018).
[12] S. Bravyi, L. Caha, R. Movassagh, D. Nagaj, and P. W. Shor, Phys. Rev. Lett. **109**, 207202 (2012).
[13] R. Movassagh and P. W. Shor, Proc. Natl. Acad. Sci. USA **113**, 13278 (2016).
[14] O. Salberger and V. Korepin, Rev. Math. Phys. **29**, 1750031 (2017).
[15] L. Dell'Anna, O. Salberger, L. Barbiero, A. Trombettoni, and V. E. Korepin, Phys. Rev. B **94**, 155140 (2016).
[16] Z. Zhang, A. Ahmadain, and I. Klich, Proc. Natl. Acad. Sci. USA **114**, 5142 (2017).
[17] X. Chen, E. Fradkin, and W. Witczak-Krempa, J. Phys. A **50**, 464002 (2017).
[18] O. Salberger, P. Padmanabhan, and V. Korepin, arXiv:1809.00709.
[19] F. G. Brandao, E. Crosson, M. B. Şahinoğlu, and J. Bowen, Phys. Rev. Lett. **123**, 110502 (2019).
[20] G. Vitagliano, A. Riera, and J. Latorre, New J. Phys. **12**, 113049 (2010).
[21] G. Ramírez, J. Rodríguez-Laguna, and G. Sierra, J. Stat. Mech.: Theory Exp. (2014) P10004.
[22] E. Tonni, J. Rodríguez-Laguna, and G. Sierra, J. Stat. Mech.: Theory Exp. (2018) 043105.
[23] V. Alba, S. N. Santalla, P. Ruggiero, J. Rodriguez-Laguna, P. Calabrese, and G. Sierra, J. Stat. Mech.: Theory Exp. (2019) 023105.
[24] O. Salberger, T. Udagawa, Z. Zhang, H. Katsura, I. Klich, and V. Korepin, J. Stat. Mech.: Theory Exp. (2017) 063103.
[25] Z. Zhang and I. Klich, J. Phys. A **50**, 425201 (2017).
[26] T. Udagawa and H. Katsura, J. Phys. A **50**, 405002 (2017).
[27] J. P. Garrahan, A. Stannard, M. O. Blunt, and P. H. Beton, Proc. Natl. Acad. Sci. **106**, 15209 (2009).
[28] I. Klich, S.-H. Lee, and K. Iida, Nat. Commun. **5**, 3497 (2014).
[29] G. Evenbly and G. Vidal, J. Stat. Phys. **145**, 891 (2011).
[30] S. Ryu and T. Takayanagi, Phys. Rev. Lett. **96**, 181602 (2006).
[31] R. Movassagh, J. Math. Phys. **58**, 031901 (2017).
[32] J. Maldacena and L. Susskind, Fortschr. Phys. **61**, 781 (2013).
[33] K. Jensen and A. Karch, Phys. Rev. Lett. **111**, 211602 (2013).